

Wind loads on a moving vehicle–bridge deck system by wind-tunnel model test

Yongle Li^{*1}, Peng Hu^{1a}, You-Lin Xu², Mingjin Zhang¹ and Haili Liao¹

¹Department of Bridge Engineering, Southwest Jiaotong University, Chengdu, Sichuan 610031, China

²Department of Civil and Environmental Engineering, The Hong Kong Polytechnic University, Hong Kong

(Received April 19, 2014, Revised June 8, 2014, Accepted June 16, 2014)

Abstract. Wind-vehicle-bridge (WVB) interaction can be regarded as a coupled vibration system. Aerodynamic forces and moment on vehicles and bridge decks play an important role in the vibration analysis of the coupled WVB system. High-speed vehicle motion has certain effects on the aerodynamic characteristics of a vehicle-bridge system under crosswinds, but it is not taken into account in most previous studies. In this study, a new testing system with a moving vehicle model was developed to directly measure the aerodynamic forces and moment on the vehicle and bridge deck when the vehicle model moved on the bridge deck under crosswinds in a large wind tunnel. The testing system, with a total length of 18.0 m, consisted of three main parts: vehicle-bridge model system, motion system and signal measuring system. The wind speed, vehicle speed, test objects and relative position of the vehicle to the bridge deck could be easily altered for different test cases. The aerodynamic forces and moment on the moving vehicle and bridge deck were measured utilizing the new testing system. The effects of the vehicle speed, wind yaw angle, rail track position and vehicle type on the aerodynamic characteristics of the vehicle and bridge deck were investigated. In addition, a data processing method was proposed according to the characteristics of the dynamic testing signals to determine the variations of aerodynamic forces and moment on the moving vehicle and bridge deck. Three-car and single-car models were employed as the moving rail vehicle model and road vehicle model, respectively. The results indicate that the drag and lift coefficients of the vehicle tend to increase with the increase of the vehicle speed and the decrease of the resultant wind yaw angle and that the vehicle speed has more significant effect on the aerodynamic coefficients of the single-car model than on those of the three-car model. This study also reveals that the aerodynamic coefficients of the vehicle and bridge deck are strongly influenced by the rail track positions, while the aerodynamic coefficients of the bridge deck are insensitive to the vehicle speed or resultant wind yaw angle.

Keywords: crosswinds; moving-vehicle model; wind loads; wind-tunnel test; wind-vehicle-bridge system

1. Introduction

When a vehicle is moving on a bridge deck under crosswinds, the wind relative to the vehicle is the resultant of the incident crosswind and the wind due to the vehicle velocity, as shown in Fig. 1. The velocity of the wind due to the vehicle motion is equal to the vehicle velocity in the magnitude

*Corresponding author, Professor, E-mail: lele@swjtu.edu.cn

^a Ph.D., E-mail: hupengmail@126.com

but opposite in direction. During the course of the vehicle motion, aerodynamic characteristics of the vehicle would be influenced by the three-dimensional ambient flow around the vehicle body due to the squeezing action on the vehicle nose and the end trailing action over the air flow. Significant aerodynamic interaction between the moving vehicle and the bridge deck exists under crosswinds. On the one hand, the existence of the vehicle on the bridge deck changes the aerodynamic ambient flow around the bridge deck, and the aerodynamic characteristics and wind loads on the bridge deck vary with the vehicle arrival and departure dynamically; on the other hand, since the vehicle is submerged in the ambient flow around the bridge deck, the geometric shape of the bridge deck would influence the wind loads acting on the vehicle. In the analysis of the coupled vehicle-bridge vibration, the vehicle and bridge deck are usually regarded as two independent dynamic subsystems, satisfying some coupling relationship with the iterative method; when considering the crosswind actions, the aerodynamic parameters of the vehicle and bridge deck are required in vehicle-bridge coupling vibration analysis (Li *et al.* 2005, Xu and Guo 2003, Cai and Chen 2004), and the effects of vehicle motion and aerodynamic interaction between the vehicle and the bridge deck should also be taken into account.

Aerodynamic parameters of a vehicle-bridge system are obtained mainly from either wind tunnel tests or numerical simulations through computational fluid dynamics (CFD). For the CFD numerical simulation of the two-dimensional ambient flow around a vehicle-bridge system, the computational cost is relatively less and the system parameters could be readily adjusted (Zhu and Chen 2001), such as the wind speed, wind attack angle, vehicle type, bridge type and relative position of the vehicle to the bridge deck, but it is difficult to consider the effects of the vehicle motion. CFD numerical simulation of the three-dimensional ambient flow can consider the effects of the vehicle motion and the interaction between the vehicle and the bridge deck by using multi-reference frame method (Huang *et al.* 2006), mixing plane method or sliding mesh method. However it involves a high computing cost and the computational precision needs to be validated.

Most of the previous wind tunnel tests studying on aerodynamic parameters were performed on either vehicles or bridge decks, and only a limited number of investigations on the aerodynamic interaction between them were performed. Among these studies with the consideration of the interaction between vehicles and bridge decks, some researchers only measured the aerodynamic coefficients of the vehicle (Suzuki *et al.* 2003, Yang *et al.* 2008) or on the bridge deck (Zhou and Ge 2008). Li *et al.* (2004) conducted a series of wind tunnel tests utilizing a combined section model to simulate the aerodynamic interaction between a vehicle and a bridge deck, and measured the aerodynamic forces and moment on the vehicle and bridge deck, respectively. Furthermore, the effects of vehicle motion were approximately considered by the cosine rule (Chiu and Squire 1992).

Enhanced by the construction of high-speed railways and the constantly increasing vehicle speeds, the effects of the motion of a vehicle running along a bridge deck on the aerodynamic characteristics of the vehicle-bridge system are attracting widespread attention in the field. Since the bridge deck is almost stationary when the vehicle is moving forward on the bridge deck, the wind directions relative to the vehicle and to the bridge deck are different. Therefore, it may be problematic to consider the effects of the moving vehicle by setting the wind yaw angle of the vehicle-bridge model in the WVB system (Chiu 1995, Zhang and Chen 1998). In order to consider the aerodynamic effects of the moving vehicle, British Railways Board (Pope 1991) developed a moving vehicle model facility with the power plant provided by a rubber band launcher to mainly study the longitudinal resistance and vertical lift. Charuvisit *et al.* (2004) studied the aerodynamic forces on moving road vehicles when they passed through a bridge tower through wind tunnel tests,

but the vehicle running path was so short in total that only the side force and yawing moment were obtained from the tests. Baker (1986) measured the aerodynamic forces on a rail vehicle by a moving vehicle model test in an atmospheric boundary layer wind tunnel, and described the experimental difficulties involved and difficulties in interpreting the results. Previous moving vehicle model tests remains deficient for taking the interaction between moving vehicles and bridge decks into consideration or measuring their respective aerodynamic forces simultaneously.

To comprehensively consider the effects of moving vehicles and the aerodynamic interaction between moving vehicles and bridge decks, a new testing system was developed by the authors in this paper: a wind tunnel test rig with a moving vehicle model (this new testing system was briefly introduced by Li *et al.* (2013)). The new testing system made full use of a large wind tunnel with 22.5 m width to simultaneously measure the respective aerodynamic forces and moment on the moving vehicles and bridge decks under crosswinds. It is convenient to change the wind speed, vehicle speed, testing objects and relative position of the vehicle to the bridge deck for different test cases. By using the testing system, a three-car vehicle model corresponding to a rail vehicle (such as a train or a light rail vehicle) and a single-car vehicle model corresponding to a road vehicle (such as a truck or a car) were then designed to measure the aerodynamic forces and moment acting on the moving vehicle and bridge deck in various testing cases, addressing the effects of the vehicle speed, yaw angle, rail position of the vehicle to the bridge deck and vehicle type on the aerodynamic characteristics of the moving vehicle and bridge deck.

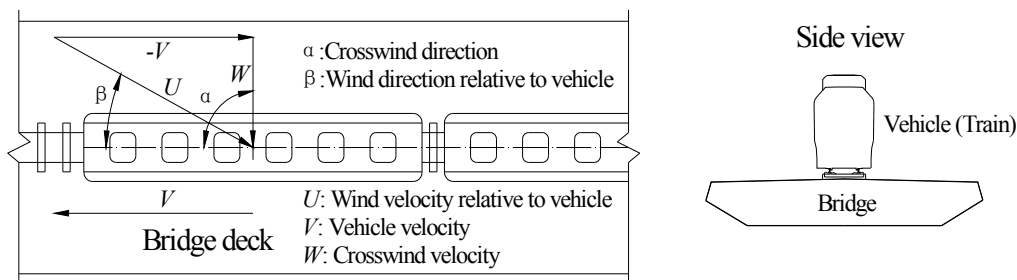


Fig. 1 Wind velocity relative to the vehicle

2. Wind tunnel test rig with moving vehicle model

The wind tunnel tests were conducted in the XNJD-3 wind tunnel of Southwest Jiaotong University. The wind tunnel has a test section with 22.5 m in width, 36.0 m in length, and 4.5 m in height. Taking advantage of the large width of the XNJD-3 wind tunnel, a new testing system with a moving vehicle model was developed (shown in Fig. 2) to simultaneously measure the respective aerodynamic forces and moment on the moving vehicle and the bridge deck when the vehicle model is moving on the bridge deck under crosswinds. The whole set of test equipment mainly includes three components: vehicle-bridge model system, motion system and signal measuring system. The test equipment with a total length of 18.0 m was placed perpendicular to the flow direction in the XNJD-3 wind tunnel test section.

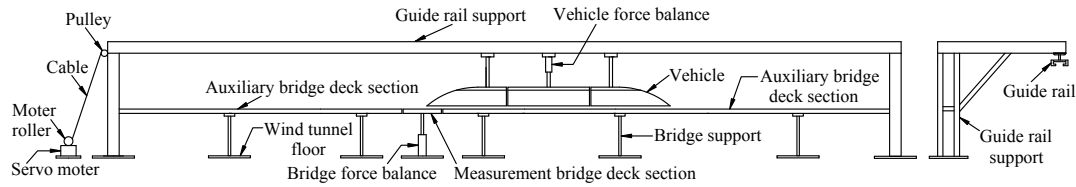


Fig. 2 Schematic diagram of the testing system

2.1 Vehicle-bridge model system

Considering the factors such as the test section size of the wind tunnel, the motion time of the moving vehicle and others, geometrical scaled models of the vehicle and bridge were decided. In order to reduce the influence of the inertial effects when the vehicle model accelerated or decelerated, the mass of the vehicle model should be as light as possible, so the hollow light wood was used to simulate the general outline of the vehicle model. The three-car vehicle model shown in Fig. 3 was adopted for a rail vehicle, and the length of each car model is 0.5 m. The middle car was used to simulate the middle part of a train, and the front and rear parts were used to simulate the front car and end car of a train, respectively. For the middle car, the front car and end car were provided as the transition section of aerodynamic forces to weaken the effects of the three-dimensional ambient flow around the front and end of the train. As a result, the aerodynamic forces and moment acting on the middle car are more stable, so just the middle car was instrumented in this study. For a road vehicle such as a truck or a car, a single-car or two-car (i.e., a car with a trailer) vehicle model was enough to meet the demand. As vehicle wheels have a small windproof effect, they were not simulated in the vehicle-bridge model system. The vehicle model and bridge model were separated from each other by a small gap, which indicates the space between the train body and the bridge deck in reality. The total length of the bridge deck model was 13.07 m with a constant section, and the measurement bridge deck section with 0.5 m in length was set at 8.38 m. Two auxiliary bridge deck sections were set on the both sides of the measurement bridge deck section, as shown in Fig. 2. Auxiliary bridge deck sections were employed to simulate the effects of the bridge deck on the ambient flow around the vehicle, while the measurement bridge deck section was used to measure the aerodynamic coefficients of the bridge deck.

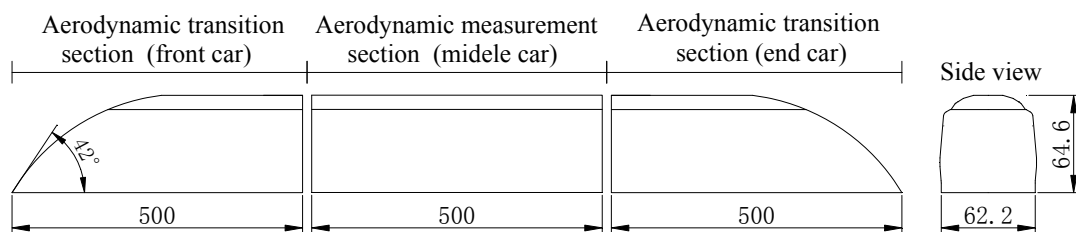


Fig. 3 Schematic diagram of the three-car vehicle model (Unit: mm)

2.2 Motion system

The motion system consisted of four parts: guide rail, sliding element, driving motor and buffer device. The total length of the guide rail with a continuously smooth sliding slot was 18.0 m. In order to decrease the guide rail deformation and increase the running stability of the vehicle model, the guide rail was made very rigid. The sliding element was composed of slide blocks and a bidirectional conversion bracket. The slide blocks were installed on the bidirectional conversion bracket, and the vehicle model was connected to the bidirectional conversion bracket through connecting parts. As a result, the vehicle model and the slide blocks were united together and could run along the guide rail flexibly, as shown in Fig. 4. The bidirectional conversion bracket was designed to conveniently adjust the vehicle length, vehicle numbers and relative positions of the vehicle to the bridge deck in the horizontal and vertical directions and so on. The different rail track positions on the bridge deck are shown in Fig. 5. A servo motor was employed to drive the vehicle by pulling a cable, and the motor roller was linked to the sliding blocks through the cable (shown in Fig. 2). The motor could accelerate to a preset speed and stay constant when the acceleration was completed. Therefore, different vehicle speeds could be conveniently set by adjusting the motor roller speed. In order to avoid the cable overlapping when convolving around the motor roller, the motor roller could also have translational motion at the same time of rotation. For the different vehicle speed cases, the same operation was adopted with the initial 4.5 m of the guide rail as the vehicle acceleration section, the intermediate 9.0 m as the uniform motion section and the last 4.5 m as deceleration to stop section. In order to avoid the damage of the vehicle force balance (shown in Fig. 2) due to the excessive inertia force, rubber block cables and collision sponges were used to make the vehicle decelerate slightly.

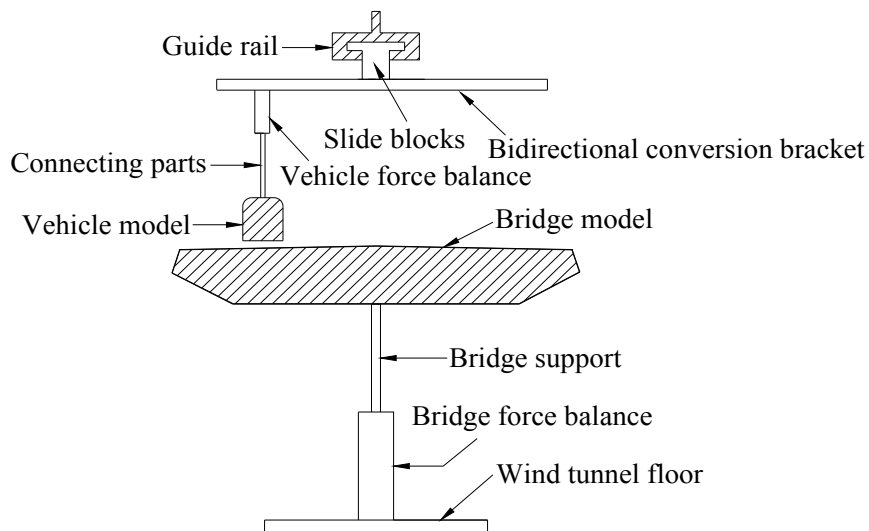


Fig. 4 Transversal arrangement of the vehicle and bridge deck models

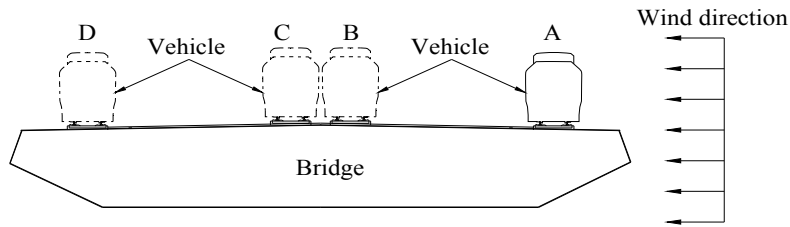


Fig. 5 Different rail track positions on the bridge deck

2.3 Signal measuring system

The signal measuring system included both force balances and data acquisition devices. Two force balances were employed to measure the aerodynamic forces and moment on the vehicle and the bridge deck, respectively. One of the force balances was linked to the middle car model by connecting parts, thus they could move along the guide rail together. For the three-car vehicle model, only the middle car was of concern in the test. Then the front car, middle car and end car were separated from each other (shown identified in Fig. 3) to ensure that the vehicle force balance only measured the aerodynamic forces and moment acting on the middle car. The other force balance was employed to measure the aerodynamic forces and moment on the bridge deck, and it was linked to the wind tunnel floor at one end and the measurement bridge deck section at the other end, respectively, as shown in Fig. 4. The measurement bridge deck section was also separated from the two auxiliary bridge deck sections to ensure that the bridge force balance only measured the aerodynamic forces and moment acting on the measurement bridge deck section. When the vehicle model was moving on the auxiliary bridge deck sections, the bridge force balance measured the aerodynamic forces and moment on the measurement bridge deck section without the vehicle, while the vehicle model was moving above the measurement bridge deck section, the bridge force balance measured the aerodynamic forces and moment on the vehicle-bridge system. The relative position of the three-car vehicle model to the bridge deck sections in the longitudinal direction is shown in Fig. 6.

The six-component balance with a full measurement range of 10N was used to measure the aerodynamic forces and moment on the vehicle model, and the five-component balance with a full measurement range of 50 N was used to measure the aerodynamic forces and moment on the bridge deck model. The data acquisition device with 11 channels could simultaneously collect the signals from the two force balances. Data post-processing was carried out by a self-written computer program.

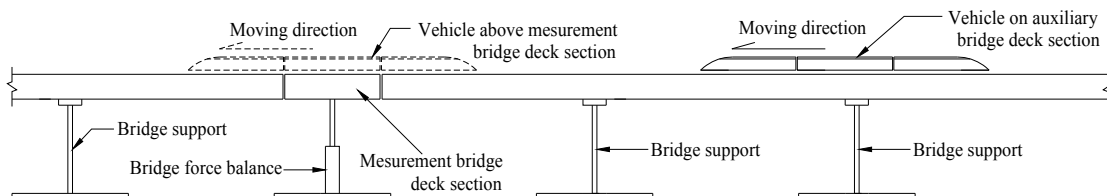


Fig. 6 Relative position of the vehicle model to the bridge deck sections in the longitudinal direction

3. Data processing and analysis

3.1 Aerodynamic force and moment coefficients

In this study, the aerodynamic force and moment coefficients of the vehicle and bridge deck were defined as follows:

Drag coefficient

$$C_{H,i} = \frac{F_{H,i}}{\frac{1}{2}\rho V^2 H_i L_i} \quad (1)$$

Lift coefficient

$$C_{V,i} = \frac{F_{V,i}}{\frac{1}{2}\rho V^2 B_i L_i} \quad (2)$$

Moment coefficient

$$C_{M,i} = \frac{F_{M,i}}{\frac{1}{2}\rho V^2 B_i^2 L_i} \quad (3)$$

where $1/2\rho V^2$ is the dynamic pressure of wind; V is the incident wind speed; ρ is the air density; H_i , B_i and L_i ($i = V$ and B) are the height, width and length of the vehicle and bridge deck, respectively; $F_{H,i}$, $F_{V,i}$ and $F_{M,i}$ represent their respective drag force, lift force and moment, and the positive values of the force and moment vectors are defined in Fig. 7; $C_{H,i}$, $C_{V,i}$ and $C_{M,i}$ represent their respective drag coefficient, lift coefficient and moment coefficient.

Aerodynamic forces and moments were measured by force balances, and then the aerodynamic coefficients of the vehicle and bridge deck could be obtained using Eqs. (1)-(3). In addition, in order to improve the signal reliability and eliminate the noise signals, a double-averaging method was introduced as described in Section 3.2.

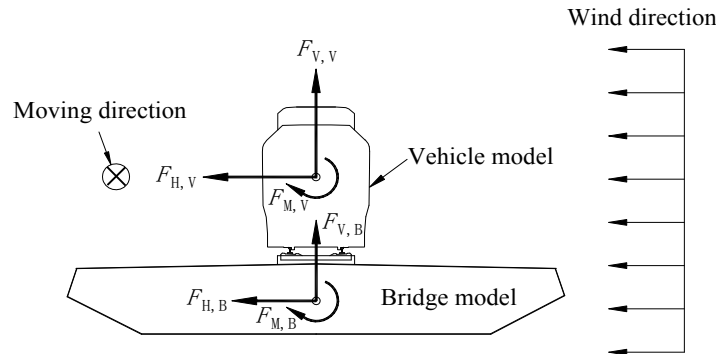


Fig. 7 Definition of the aerodynamic forces and moment acting on the vehicle and bridge deck

3.2 Signal processing for the aerodynamic forces and moment on the vehicle

Signal processing method for dynamic signals is one of the difficult points for moving vehicle model tests (Baker 1986). When the vehicle model is moving on the bridge deck at a high speed, various interference factors, such as the vehicle model vibration, bidirectional conversion bracket vibration, guide rail irregularity and inertial force caused by the vehicle model speed variation, can cause obvious noise signals, and there will be a large error if the aerodynamic forces and moment are calculated directly based on the original signals. Therefore, all the aerodynamic coefficients were filtered using a low-pass filter at a cutting frequency of 4 Hz (MathWorks Inc. 2005, Li *et al.* 2013). To better clarify the processing method for aerodynamic force and moment signals, a typical case with a wind speed of 8 m/s, a vehicle speed of 6 m/s and the three-car vehicle model was considered as an example. It should be noted that only the aerodynamic forces and moment on the middle car were measured for the three-car vehicle model, as shown in Fig. 3.

The longitudinal inertial force of the vehicle model is zero when the vehicle model is static or moves uniformly at a constant velocity. Once the vehicle model begins to move, the longitudinal inertial force will increase rapidly due to the drive of the cable by the servo motor. Therefore, the time when the vehicle model begins to move can be determined from the time history curve of the longitudinal force coefficient (corresponding to the longitudinal inertial force, of which definition is similar to Eq. (2)). Then the stages of acceleration, uniform motion and deceleration to stop all can be derived from the acceleration distance and the speed and distance of vehicle model in the uniform motion. As shown in Fig. 8, the longitudinal inertial force is almost zero before the vehicle model starts to move. In the acceleration section, the longitudinal inertial force increases rapidly at first and then obviously fluctuates, probably for the non-uniform speed-up of the vehicle model caused by the weight of the model itself, and the elastic stretch and sag of the cable. In the uniform motion section, the time history curve of the longitudinal inertial force coefficient has a descent stage because the vehicle acceleration changes from a certain value to zero. Moreover, the longitudinal inertial force still fluctuates in this section due to the influences of cable and the vibration of the vehicle model. In the deceleration to stop section, the vehicle model decelerates rapidly due to the blocking effect of rubber cables and sponges, and the data in this section have no physical meanings. If the vehicle aerodynamic force and moment coefficients were derived directly from the signal data in the uniform motion section, there would still be a large error. At this juncture, a better section, here called the stable section, could be extracted from the uniform motion section, in which the average of longitudinal inertial force is about zero. As shown in Fig. 8, the time history curve of the longitudinal force coefficient in the stable section fluctuates around the zero value. It is clear that the curve stability in the stable section is better than that in the whole uniform motion section. Since the signals of all force components of the vehicle force balance are measured simultaneously, the stable section of other force components can be determined according to the beginning time and ending time of the stable section of the longitudinal force coefficient. The stable section of the vehicle drag coefficient is shown in Fig. 9. It shows that the curve in the stable section is indeed more stable than that in the whole uniform motion section. Therefore, only the data of stable section was selected in the following analysis. The stable section of lift coefficient and moment coefficient could be obtained in the same way.

In order to improve the reliability of the aerodynamic force and moment signals, the tests were carried out repeatedly many times for each testing case. The double-averaging method was then used to determine the aerodynamic coefficients of each testing case, i.e., taking the average of all instantaneous values at the stable section of each test as the result of this test, and then taking the

average of the results of all repeated tests as the final values of aerodynamic coefficients of this testing case. If necessary, the time history curve with the average of the stable section data closer to the final value of the corresponding testing case could be chosen as the representative time history curve for this testing case. In order to describe the aerodynamic characteristics of vehicle in the stable section intuitively, the abscissa could be converted from vehicle moving time to the moving distance based on the corresponding vehicle speed. The vehicle aerodynamic force and moment coefficients with moving distance in the stable section are shown in Fig. 10, in which the corresponding length of stable section is 5.0 m. This figure shows that both the vehicle drag coefficient and moment coefficient curves are relatively stable, while the vehicle lift coefficient curve has a decline trend. The vehicle lift has a very close relationship with the ambient flow induced by the vehicle motion. When the vehicle speeds up from zero to the setting value in a short time, the ambient flow induced by the vehicle motion has not reached a steady state yet. This may be the reason why the vehicle lift coefficient curve is not stable in Fig. 10. In the analysis of the WVB coupled vibration system, the vehicle drag force and moment are more important than the lift force, then the influences of the lift force fluctuation may be relatively limited.

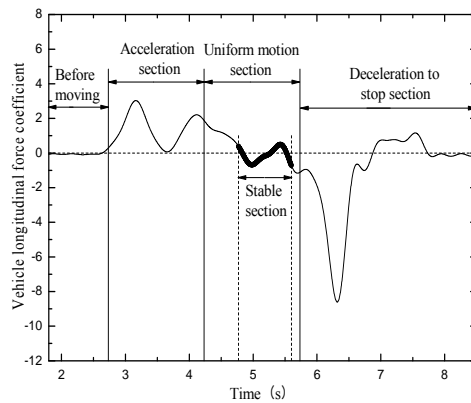


Fig. 8 Time history curve of the vehicle longitudinal force coefficient (after filtering)

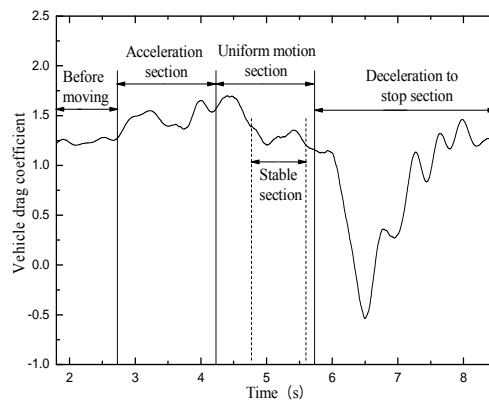


Fig. 9 Stable section of the vehicle drag coefficient

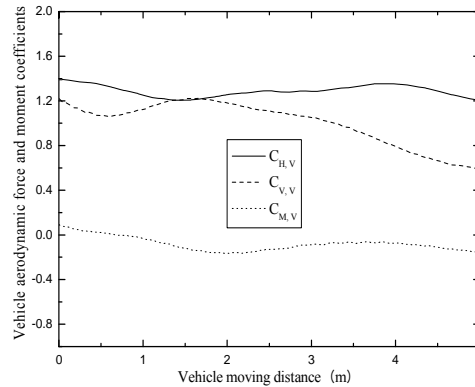


Fig. 10 Stable section of the vehicle aerodynamic force and moment coefficients

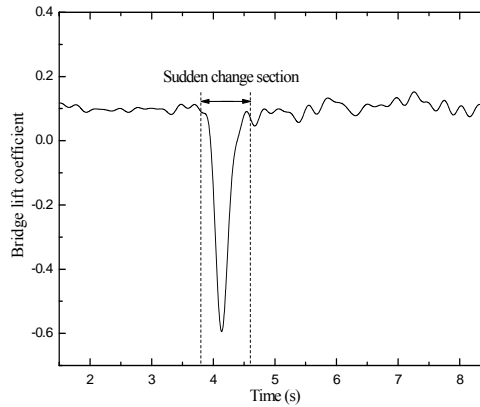


Fig. 11 Time history curve of the bridge lift coefficient (after filtering)

3.3 Signal processing for the aerodynamic forces and moment on the bridge deck

When the vehicle model is passing through the measurement bridge deck section under crosswinds, the aerodynamic forces and moment on the measurement bridge deck section have a sudden change with the vehicle arrival and departure. Fig. 11 shows the filtered time history curve of lift coefficient of the measurement bridge deck section, in which a sudden change occurs at the time of 3.8s to 4.6s. The reason is that the ambient flow around the measurement bridge deck section is changed in the process of the vehicle arrival and departure.

Converting the abscissa in Fig. 11 from the vehicle moving time to the vehicle moving distance based on the vehicle speed and considering the changes of the bridge aerodynamic force and moment coefficients with the vehicle passing through the measurement bridge deck section, a suitable length of the lift coefficient time history curve was selected, as shown in Fig. 12. Then, the maximum point of the time history curve was identified by a computer program, and regarded as the result of the bridge lift coefficient for this test. Here, noting that for the real life of vehicle moving along the bridge deck, the bridge lift coefficient should be more stable, but both of the

values in the real life and in the test should be almost the same. Therefore, for the real world, the bridge lift coefficient in the vehicle-bridge system can be obtained by extending the minimum value in Fig. 11 or Fig. 12 to form a time history. Certainly, in order to reduce errors, the above tests should be carried out several times repeatedly for each testing case, and finally the average of the results of all repeated tests is taken as the final value of this testing case. The same processing method was applied to the determination of the bridge drag coefficient and moment coefficient.

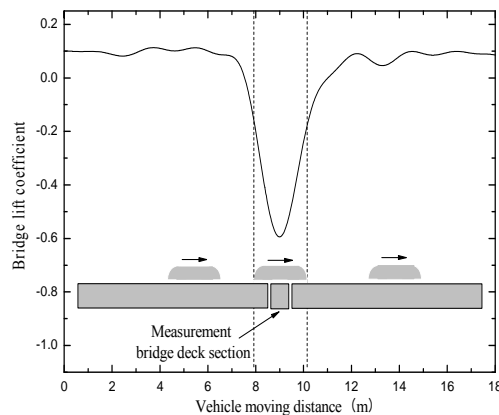


Fig. 12 Time history curve of the bridge lift coefficient when the vehicle passes through the measurement bridge deck section

4. Dynamic tests of moving vehicle and bridge deck

Both the vehicle model and bridge model were in the length scale of 1:45. Since the bridge adopted in this study was a light-railway and highway bridge, it was necessary to investigate the aerodynamic characteristics of both the rail vehicles and road vehicles in the study. As a result, a three-car vehicle model and a single-car vehicle model were employed to simulate the rail vehicles and road vehicles, respectively. It is noted that the three-car vehicle model was adopted for rail vehicles, but only the middle car was measured in the test, with the front car and end car provided as the aerodynamic transition sections, as shown in Fig. 3. For road vehicles, in order to reveal the aerodynamic transition effects of the front car and end car, the middle car in the three-car vehicle model was directly taken as the single-car vehicle model in the test. In addition, the rail tracks of A, B, C and D were set on the bridge deck, as shown in Fig. 5. The vehicle model moved along these rail tracks and the effects of different rail track positions on the aerodynamic characteristics of the vehicle and bridge deck could be investigated. In the present study, the uniform flow with low turbulence intensity was adopted, and the wind speeds of 6 m/s, 8 m/s and 10 m/s were set in the wind tunnel tests, corresponding to the Reynolds numbers, Re , of 6×10^5 , 8×10^5 and 10^6 (defined by the length of the three-car vehicle model), respectively. It is usually difficult to exactly match Re number between the model and prototype in the conventional wind tunnels. Furthermore, the Re numbers were not too low and this paper concerns about the aerodynamic mechanism more than the practical applications. Therefore, the effects of Re were not considered enough in the study. Four different vehicle speeds including 0 m/s, 4 m/s, 6 m/s and 8 m/s were adopted in the

test. For the sake of data processing analysis for different vehicle speeds, the length of the data acquisition time was 12s, and the sampling frequency was 909 Hz, which were adequate for all the test cases. Since the dynamic test data in each repeated test were generally close, with consideration of the total number of test cases and testing cost, the test was repeatedly carried out five times for each testing case. Fig. 13 shows the five stable section curves of the vehicle drag coefficient with the typical case using in Section 3.2. It can be seen from the figure that the differences between the five stable section curves are really small, which are unlikely to cause significant errors. Furthermore, the average value of the first stable section data are closer to the final value of the total five stable section data. As discussed earlier, the first stable section time history curve was chosen as the representative time history curve for this test case, as shown in Fig. 10. Certainly, similar processing method is applied to the lift and moment coefficients of the vehicle and also applied to the aerodynamic coefficients of the bridge deck. Then the time histories given in this paper should have a relatively high degree of reliability by the above proceeding.

As described in the following sections, to comprehensively investigate the effects of some factors such as the vehicle speed, wind yaw angle and rail track positions on the aerodynamic characteristics of the moving vehicle and bridge deck, the corresponding testing cases were conducted and the test results are analyzed. For the sake of convenience, the “vehicle aerodynamic forces and moment” just refers to the aerodynamic forces and moments acting on the middle car in the three-car vehicle model (or the single-car vehicle model for road vehicles), and the “bridge aerodynamic forces and moment” just refers to aerodynamic forces and moment acting on the measurement bridge deck section in this paper. The same terminology is applied to “vehicle aerodynamic force and moment coefficients” and “bridge aerodynamic force and moment coefficients”.

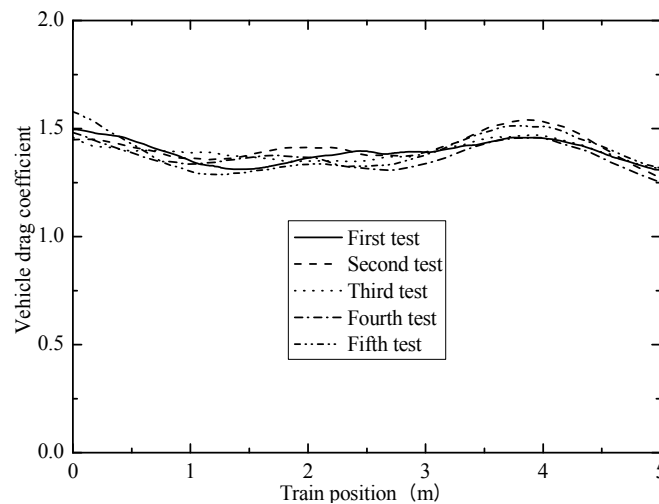


Fig. 13 Five stable section curves of the vehicle drag coefficient

4.1 Effects of vehicle speed

4.1.1 Three-car vehicle model

In order to investigate the effects of different vehicle speeds on the aerodynamic forces and moment on the vehicle and bridge deck, the testing cases of the three-car vehicle model moving along the windward rail track A were conducted at the wind speed of 10 m/s and vehicle speed of 0 m/s, 4 m/s, 6 m/s and 8 m/s, respectively. The vehicle aerodynamic force and moment coefficient time histories of the stable section at different vehicle speeds are shown in Figs. 14-16. The time history curves all fluctuate in some degree mainly because of the test device vibration and non-uniform vehicle speed. There are some differences in the vehicle drag coefficient time histories at different vehicle speeds, but the differences are not obvious. Note that, compared to the static vehicle (corresponding to the vehicle speed of 0 m/s), the lift coefficients of the moving vehicle become significantly larger than those of the static vehicle. The reason is that a negative pressure zone occurs over the moving vehicle roof due to a flow separation induced by the nose of the front car (Hemida and Krajnović 2010, Li *et al.* 2011). In addition, all time history curves of the vehicle lift coefficient at various vehicle speeds have a declining trend. The main reason is that the vehicle lift has a very close relationship with the ambient flow induced by the vehicle motion, and the ambient flow has not yet reached a steady state during the process of vehicle speed increasing from zero to the setting value in such a short time. The vehicle moment coefficients at different vehicle speeds have an incremental trend, but the change is not obvious. The bridge aerodynamic force and moment coefficient time histories at various vehicle speeds are shown in Figs. 17-19. When the vehicle model does not reach the measurement bridge deck section, the bridge aerodynamic force and moment coefficients are close to each other at different vehicle speeds. However, when the vehicle model moves above the measurement bridge deck section (corresponding to the abscissa range from 5.25 to 6.75 m), the bridge drag and lift coefficients sharply decrease while the moment coefficients obviously increase. Therefore, it can be concluded that the existence of vehicle has a significant influence on the bridge aerodynamic force and moment coefficients.

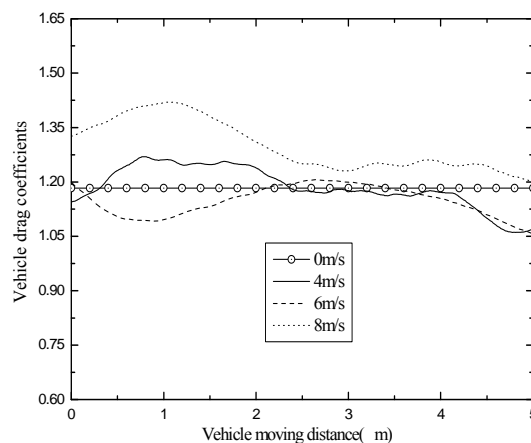


Fig. 14 Time histories of the vehicle drag coefficients at different vehicle speeds

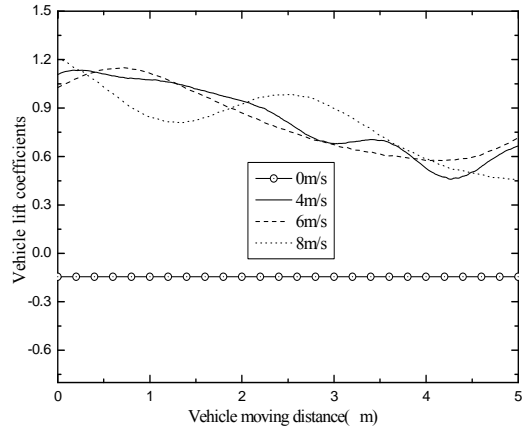


Fig. 15 Time histories of the vehicle lift coefficients at different vehicle speeds

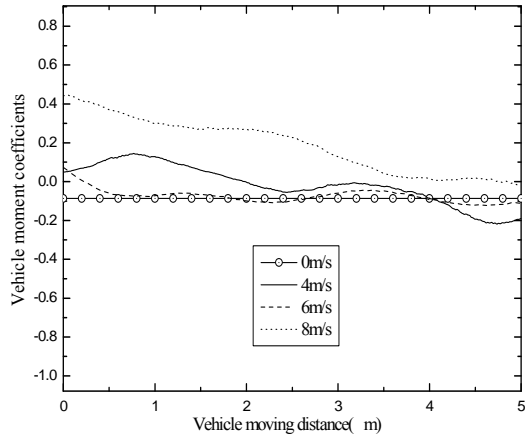


Fig. 16 Time histories of the vehicle moment coefficient at different vehicle speeds

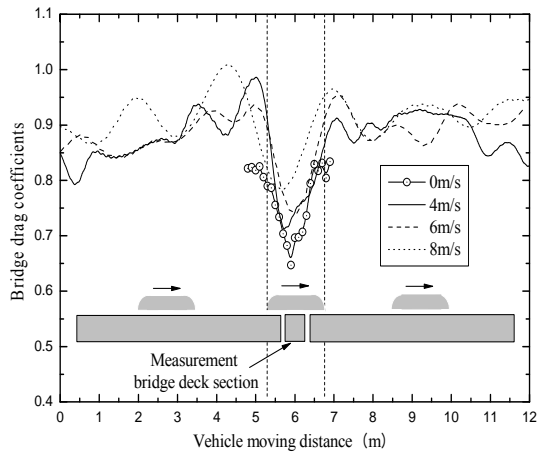


Fig. 17 Time histories of the bridge drag coefficient at different vehicle speeds

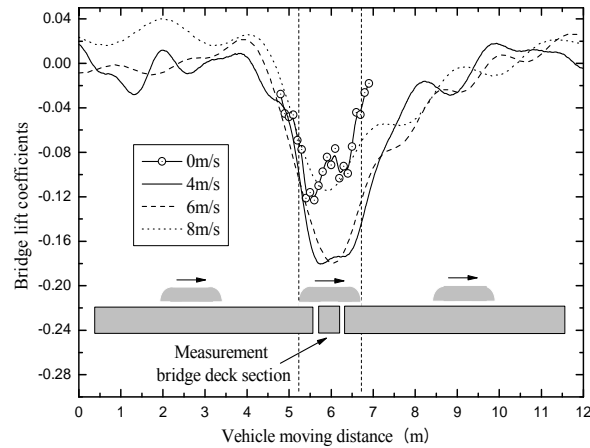


Fig. 18 Time histories of the bridge lift coefficient at different vehicle speeds

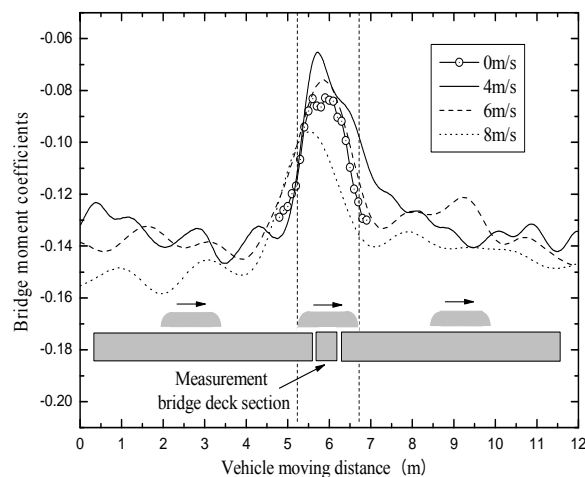


Fig. 19 Time histories of the bridge moment coefficient at different vehicle speeds

The final values of the aerodynamic force and moment coefficients of the vehicle and bridge are shown in Table 1. The vehicle lift coefficients are all negative when vehicle is static (i.e., the vehicle speed is zero), while they turn positive when vehicle moves at a certain speed, which indicates that the vehicle motion has a great effect on the vehicle lift coefficient. The change of vehicle drag and moment coefficients with the vehicle speed is not unexpected, and the reason may be that the ambient flow around the middle car is relatively stable because of the aerodynamic transition effect of the front car and end car, and the cross section of the vehicle model is relatively regular, which makes the influence of three-dimensional ambient flow induced by the vehicle motion limited. Moreover, the bridge drag coefficient has an incremental trend with the increase of vehicle speed, but the bridge lift and moment coefficients are not sensitive to the vehicle speeds.

Table1 Final values of the vehicle and the bridge aerodynamic force and moment coefficients (three-car vehicle model)

| | Vehicle speed (m/s) | C_H | C_V | C_M |
|---|---------------------|--------|---------|---------|
| Vehicle aerodynamic force and moment coefficients | 0.0 | 1.1827 | -0.1444 | -0.0867 |
| | 4.0 | 1.1768 | 0.8184 | -0.0188 |
| | 6.0 | 1.1442 | 0.8440 | -0.0733 |
| | 8.0 | 1.2450 | 0.7800 | 0.1023 |
| Bridge aerodynamic force and moment coefficients | 0.0 | 0.6876 | -0.1215 | -0.0854 |
| | 4.0 | 0.7219 | -0.1583 | -0.0720 |
| | 6.0 | 0.7304 | -0.1442 | -0.0802 |
| | 8.0 | 0.7611 | -0.1409 | -0.0879 |

4.1.2 Single-car vehicle model

In this study, the three-car vehicle model represented rail vehicles such as a train or a light rail vehicle, while the single-car vehicle model represented a road vehicle such as a truck or a car. In order to investigate the influences of different vehicle speeds on the aerodynamic forces and moment on the vehicle and bridge deck, the testing cases of the single-car vehicle model moving along the windward rail track A were also conducted at a wind speed of 10 m/s and vehicle speed of 0 m/s, 4 m/s, 6 m/s and 8 m/s, respectively. The trends of the aerodynamic force and moment coefficients of the vehicle and bridge deck are similar to those of the three-car vehicle model and bridge deck. The final values of the force and moment coefficients are displayed in Table 2. It can be seen that the vehicle drag and lift coefficients increase with the vehicle speed, but the vehicle moment coefficient decreases to negative values with the increase of vehicle speed. This indicates that the vehicle aerodynamic force and moment coefficients of the single-car vehicle model are more sensitive to vehicle speed compared to those of the three-car vehicle model. In addition, when the vehicle is static, the absolute values of bridge drag and moment coefficients are larger than those when the vehicle is moving, while the absolute values of the bridge lift coefficient have an opposite trend. The influence of vehicle speed on the bridge aerodynamic force and moment coefficients is not strong.

Table2 Final values of the vehicle and the bridge aerodynamic force and moment coefficients (single-car vehicle model)

| | Vehicle speed (m/s) | C_H | C_V | C_M |
|---|---------------------|--------|---------|---------|
| Vehicle aerodynamic force and moment coefficients | 0.0 | 1.2366 | 0.0324 | 0.1354 |
| | 4.0 | 1.2571 | 0.5004 | 0.0734 |
| | 6.0 | 1.3049 | 0.7769 | -0.0267 |
| | 8.0 | 1.4372 | 0.8189 | -0.1192 |
| Bridge aerodynamic force and moment coefficients | 0.0 | 0.9789 | -0.0766 | -0.1207 |
| | 4.0 | 0.7643 | -0.1167 | -0.0928 |
| | 6.0 | 0.7149 | -0.1269 | -0.0889 |
| | 8.0 | 0.7627 | -0.1131 | -0.1000 |

4.2 Effects of wind yaw angle

4.2.1 Three-car vehicle model

When a vehicle is moving on a bridge deck under crosswinds, the wind relative to the vehicle is the resultant of crosswind and the wind due to vehicle motion (as shown in Fig. 1), but the bridge deck is not. Therefore, only the aerodynamic force and moment coefficients of the vehicle are discussed here. When the three-car vehicle model is moving along the windward rail track A at the wind speed of 6 m/s, 8 m/s and 10 m/s and vehicle speed of 4 m/s, 6 m/s and 8 m/s, respectively, the corresponding resultant wind yaw angles are shown in Table 3, and the vehicle aerodynamic force and moment coefficients varying with the resultant yaw angles are shown in Fig. 20. It can be seen from the figure that the aerodynamic force and moment coefficients of the vehicle fluctuate with the resultant yaw angles, but the fluctuations are not unexpected and the change is not obvious.

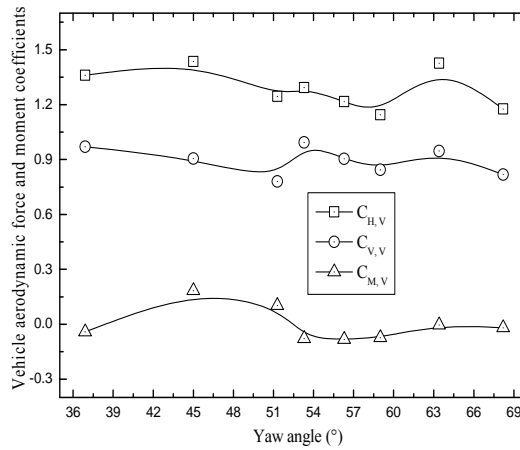


Fig. 20 Vehicle aerodynamic force and moment coefficients varying with the yaw angles (three-car vehicle model)

Table3 Resultant yaw angles (the yaw angle is 90° when the resultant wind is perpendicular to vehicle moving direction)

| Wind speeds (m/s) | Vehicle speeds (m/s) | | |
|-------------------|----------------------|-------|-------|
| | 4.0 | 6.0 | 8.0 |
| 6.0 | 56.3° | 45.0° | 36.9° |
| 8.0 | 63.4° | 53.1° | 45.0° |
| 10.0 | 68.2° | 59.0° | 51.3° |

4.2.2 Single-car vehicle model

When the single-car vehicle model is moving along the windward rail track A at various wind speeds and vehicle speeds, the vehicle aerodynamic force and moment coefficients varying with the resultant yaw angles are shown in Fig. 21. The vehicle drag and lift coefficients increase with the decrease of resultant yaw angles, which indicates that the increase of the vehicle speed can result in the increase of the vehicle drag and lift coefficients. However, the vehicle moment coefficient is not sensitive to the resultant yaw angles. Compared to the aerodynamic force and moment coefficients of the three-car vehicle model, the trends in the variation of the aerodynamic force and moment coefficients of the single-car vehicle model with the resultant yaw angles appear more obvious. It implies that the aerodynamic transition effect due to the existence of the front car and end car weakens the influences of vehicle motion on the aerodynamic force and moment of the middle car.

4.3 Effects of rail track position

4.3.1 Three-car vehicle model

In order to investigate the effects of different rail track positions on the aerodynamic forces and moment on the vehicle and bridge deck, the testing cases of the three-car vehicle model moving respectively along the four different rail tracks A, B, C and D were conducted at a wind speed of 10m/s and vehicle speed of 8 m/s. With regard to the vehicle model moving along the rail tracks A, B, C and D respectively, the final values of the vehicle and bridge aerodynamic force and moment coefficients are shown in Fig. 22. The vehicle aerodynamic force and moment coefficients all decrease in turn from the windward rail track A to the leeward rail track D, among which the vehicle moment coefficients decrease to negative values. The bridge drag coefficients increase in turn from the rail track A to D, but the bridge lift coefficients show an opposite trend to the bridge drag coefficients; the bridge moment coefficients show small changes.

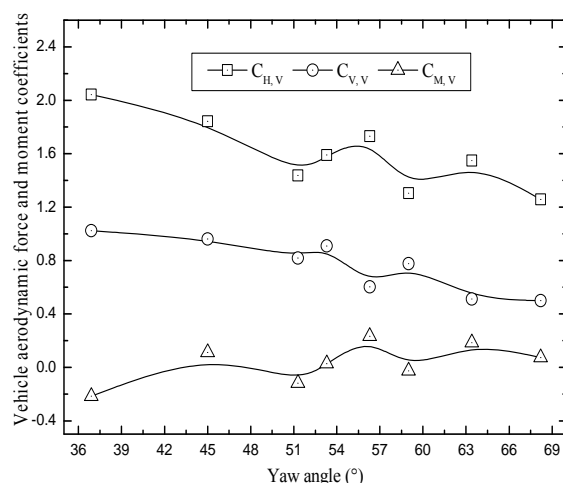


Fig. 21 Vehicle aerodynamic force and moment coefficients varying with the yaw angles (single-car vehicle model)

To further analyze the influences of different rail tracks on the aerodynamic characteristics of the bridge deck, the corresponding time histories of the bridge aerodynamic force and moment coefficients are shown in Figs. 23-25. The overall variation trends of bridge aerodynamic force and moment coefficients are similar when the vehicle model moves along the rail tracks A, B and C. Moreover, when the vehicle model moves above the measurement bridge deck section (the corresponding abscissa range from 7.25 to 8.75 m), the absolute values of both the bridge drag and moment coefficients decrease rapidly. Nevertheless, when the vehicle model moves along the rail track D, the change laws of the bridge drag and moment coefficients are not remarkable. When the vehicle model moves along the rail tracks A, B, C and D, the bridge lift coefficients are all negative values and decrease in turn.

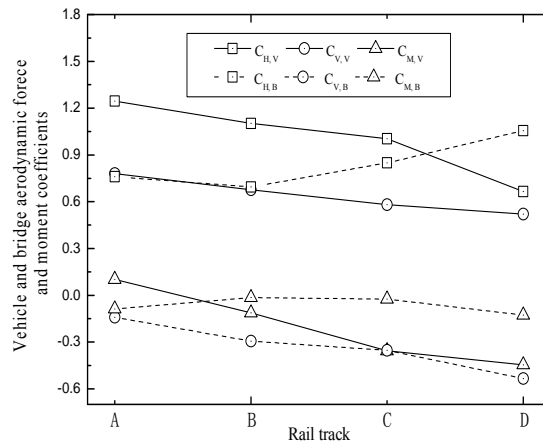


Fig. 22 Final values of the vehicle and the bridge aerodynamic force and moment coefficients for different rail track positions (three-car vehicle model)

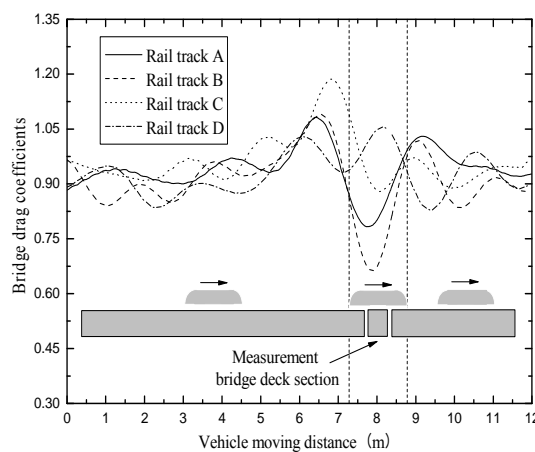


Fig. 23 Time history curves of the bridge drag coefficient for different rail positions (three-car vehicle model)

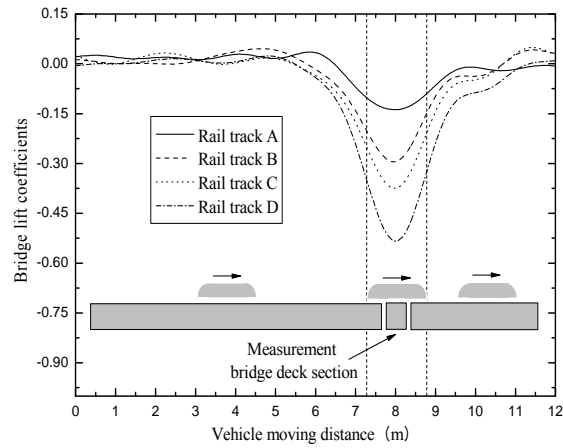


Fig. 24 Time history curves of the bridge lift coefficient for different rail positions (three-car vehicle model)

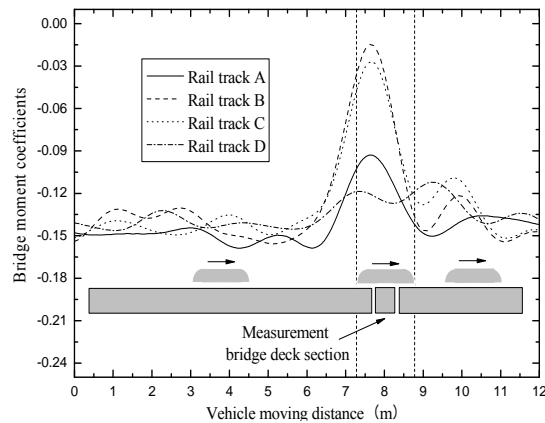


Fig. 25 Time history curves of the bridge moment coefficient for different rail positions (three-car vehicle model)

4.3.2 Single-car vehicle model

To investigate the influences of the single-car vehicle model moving along the different rail tracks on the aerodynamic forces and moment on the vehicle and bridge deck, the testing cases of the single-car vehicle model moving along two different rail tracks (i.e., windward rail track A and leeward rail track D) were conducted at a wind speed of 10m/s and vehicle speed of 8 m/s. For the same wind speed, vehicle speed and rail track position, the bridge aerodynamic force and moment coefficients for the single-car vehicle model cases showed a similar trend to those for the three-car vehicle model cases. The final values of the vehicle and the bridge aerodynamic force and moment coefficients with the vehicle model moving along the rail tracks A and D are summarized in Table 4. The drag and lift coefficients of the vehicle on the rail track A are larger than those of the

vehicle on the rail track D, and the vehicle moment coefficient becomes negative when the vehicle model moves along the rail track D. The bridge lift and moment coefficients are negative values and the absolute values increase in turn from the rail track A to D, and the bridge drag coefficient with the vehicle moving on the rail track D is larger than those with the vehicle moving on the rail track A. Generally, the single-car vehicle model shows similar trends to the three-car vehicle model.

Table4 Vehicle and bridge aerodynamic force and moment coefficients for different rail tracks (single-car vehicle model)

| Rail tracks | Test objects | C_H | C_V | C_M |
|-------------|--------------|---------|----------|----------|
| Rail track | Vehicle | 1.36939 | 0.75988 | 0.03372 |
| A | Bridge | 0.76273 | -0.11306 | -0.10004 |
| Rail track | Vehicle | 0.95797 | 0.58035 | -0.21708 |
| D | Bridge | 0.80878 | -0.30522 | -0.11662 |

5. Conclusions

This study has fully considered the effects of both the vehicle motion and the aerodynamic interaction between a moving vehicle and a bridge deck. By taking advantage of the 22.5 m wide XNJD-3 wind tunnel of Southwest Jiaotong University, a new testing system including a moving vehicle model was developed to simultaneously measure the respective aerodynamic forces and moment on a moving vehicle and bridge deck under crosswinds. It was convenient to change the wind speed, vehicle speed, test objects and relative position of the vehicle to the bridge deck in this new testing system. Not only the rail vehicles such as trains or light rail vehicles, but also road vehicles such as trucks or cars could be tested. For rail vehicles, the aerodynamic forces and moments of their front car, middle car and end car could be measured. A data processing method was also presented according to the characteristics of the time history curves of dynamic testing signals.

By using the new testing system and the corresponding data processing method, the aerodynamic force and moment coefficients of the vehicle and bridge deck were measured and analyzed for different test cases to explore the aerodynamic mechanisms of the vehicle-bridge system under crosswinds. The main conclusions are drawn as follows:

- Under crosswinds, the existence of a vehicle on the bridge deck has a significant influence on the aerodynamic force and moment coefficients of the bridge deck, but the effects of vehicle speed on the aerodynamic force and moment coefficients of the bridge deck are small.
- For the middle car in a rail vehicle (corresponding to the three-car vehicle model), the vehicle moment coefficients have an incremental trend with the increase of the vehicle speed, while the effects of vehicle speed are limited. When the vehicle moves at a certain speed, the vehicle lift coefficient becomes significantly large because of a negative pressure zone occurring over the moving vehicle roof due to a flow separation induced by the nose of the front car. For the actual train, the influences of the airflow separation on the lift force coefficient of the middle cars would

be weakened with the increase of the vehicle length.

- The change laws of the road vehicle (corresponding to the single-car vehicle model) aerodynamic force and moment coefficients with the vehicle speed are more obvious than those of the rail vehicle (corresponding to the three-car vehicle model), which shows that the aerodynamic force and moment coefficients of the road vehicle are more sensitive to vehicle speed. The vehicle drag and lift coefficients becomes greater, while its moment coefficient decreases with the increase of the vehicle speed.

- For the rail vehicles, the vehicle aerodynamic force and moment coefficients fluctuate with the resultant wind yaw angles, but there is no clear trend. For road vehicles, the vehicle drag and lift coefficients increase with the decrease of the resultant wind yaw angles. It indicates that the aerodynamic transition effect due to the existence of the front car and end car can weaken the influence of vehicle motion on the aerodynamic force and moment coefficients of the middle cars in the rail vehicles.

- For the rail vehicles and road vehicles, with vehicle position from the windward side to the leeward side, the vehicle aerodynamic force and moment coefficients decrease, and the bridge drag coefficients increase in turn, but the moment coefficients of the bridge show no obvious changes.

It should be noted that only the middle car in the rail train was measured in the present study, and the aerodynamic characteristics of the front car and end car would be much more complex and difficult to be measured.

Acknowledgements

The writers are grateful for the financial supports from the National Natural Science Foundation of China under Grant NNSF-U1334201, 50508036, and the Outstanding Young Academic Leaders Program of Sichuan Province under Grant 2009-15-406. The writers also thank the financial support from the Research Grants Council of Hong Kong through a competitive research grant (PolyU 5311/07E).

References

- Baker, C.J. (1986), "Train aerodynamic forces and moments from moving model experiments", *J. Wind Eng. Ind. Aerod.*, **24**(3), 227-251.
- Cai, C.S. and Chen, S.R. (2004), "Framework of vehicle-bridge-wind dynamic analysis", *J. Wind Eng. Ind. Aerod.*, **92**(8), 579-607.
- Charuvisit, S., Kimura, K. and Fujino Y. (2004), "Experimental and semi-analytical studies on the aerodynamic forces acting on a vehicle passing through the wake of a bridge tower in cross wind", *J. Wind Eng. Ind. Aerod.*, **92**(9), 749-780.
- Chiu, T.W. (1995), "Prediction of the aerodynamic loads on a railway train in a cross-wind at large yaw angles using an integrated two-and three-dimensional source/vortex panel method", *J. Wind Eng. Ind. Aerod.*, **57**(1), 19-39.
- Chiu, T.W. and Squire, L.C. (1992), "An experimental study of the flow over a train in a cross-wind at large yaw angles up to 90°", *J. Wind Eng. Ind. Aerod.*, **45**(1), 47-74.
- Hemida, H. and Krajnović, S. (2010), "LES study of the influence of the nose shape and yaw angles on flow structures around trains", *J. Wind Eng. Ind. Aerod.*, **98**(1), 34-46.
- Huang, L., Liao, H.L. and Li, Y.L. (2006), "Analysis of flow characteristics around train-bridge system

- under cross wind and train induced wind”, *J. Railway Sci. Eng.*, **3**(6), 61-65. (in Chinese).
- Li, Y.L., Hu, P., Cai, C.S., Zhang, M.J. and Qiang, S.Z. (2013), “Wind tunnel study of a sudden change of train wind loads due to the wind shielding effects of bridge towers and passing trains”, *J. Eng. Mech. - ASCE*, **139**(9), 1249-1259.
- Li, Y.L., Liao, H.L. and Qiang, S.Z. (2004), “Study on aerodynamic characteristics of the vehicle-bridge system by the section model wind tunnel test”, *J. China Railway Soc.*, **26**(3), 71-75. (in Chinese).
- Li, Y.L., Qiang, S.Z., Liao, H.L. and Xu, Y.L. (2005), “Dynamics of wind-rail vehicle-bridge system”, *J. Wind Eng. Ind. Aerod.*, **93**(6), 483-507.
- Li, Y.L., Wang, B., Xu, Y.L. and Liao, H.L. (2011), “Numerical simulation of aerodynamic characteristics for static and dynamic vehicle-bridge system under crosswinds”, *China Civil Eng. J.*, **44**, 87-94, (in Chinese).
- MathWorks Inc. (2005), *MATLAB 7.1.0.246 (R14)*, The MathWorks Inc, Natick, Massachusetts, USA.
- Pope, C.W. (1991), *Aerodynamics and ventilation of vehicle tunnels*, Elsevier, New York, USA.
- Suzuki, M., Tanemoto, K. and Maeda, T. (2003), “Aerodynamic characteristics of train/vehicles under cross winds”, *J. Wind Eng. Ind. Aerod.*, **91**(1-2), 209-218.
- Xu, Y.L. and Guo, W.H. (2003), “Dynamic analysis of coupled road vehicle and cable-stayed bridge systems under turbulent wind”, *Eng. Struct.*, **25**(4), 473-486.
- Yang, M.Z., Yuan, X.X., Lu, Z.J. and Huang, H.J. (2008), “Experimental study on aerodynamic characteristics of train running on Qinghai-Tibet railway under cross winds”, *J. Exper. Fluid Mech.*, **22**(1), 76-79. (in Chinese).
- Zhang, J. and Chen, N.Y. (1998), “Experimental investigations in to the effect of cross-winds on the aerodynamics of EMU vehicles”, *Electric Drive for Locomotive*, **2**, 4-6 (in Chinese).
- Zhou, L. and Ge, Y.J. (2008), “Aerodynamic coefficient of vehicle-bridge system by wind tunnel test”, *J. Harbin Inst. Technol. (New Series)*, **15**(6), 871-877.
- Zhu, Z.W. and Chen, Z.Q. (2001), “Investigation on wind loads for YZ₂₂ vehicle and railway freebeam bridge”, *J. Human University*, **28**(1), 93-97 (in Chinese).